Science Advances
AAAS

advances.sciencemag.org/cgi/content/full/7/3/eabe3778/DC1

Supplementary Materials for

Multilayered electronic transfer tattoo that can enable the crease amplification effect

Lixue Tang, Jin Shang, Xingyu Jiang*

*Corresponding author. Email: jiang@sustech.edu.cn

Published 13 January 2021, *Sci. Adv.* **7**, eabe3778 (2021)
DOI: 10.1126/sciadv.abe3778

The PDF file includes:

Other Supplementary Material for this manuscript includes the following:

(available at advances.sciencemag.org/cgi/content/full/7/3/eabe3778/DC1)

Section S1. The simulation and calculation to obtain the equation of the Crease Amplification Effect

We simplified the process of METT deforming on the creases into the model shown in fig. S1. The liquid metal-based strain sensor in the METT is printed in a linear shape. Fig. S1 top presents the stretching of the METT attached to the skin without crease from $\boldsymbol{L_0}$ to $\boldsymbol{L}$, while fig. S1 bottom presents the stretching of the METT attached to the skin with creases from $\boldsymbol{L_0}$ to $\boldsymbol{L}$. When stretching the skin without crease from $\boldsymbol{L_0}$ to $\boldsymbol{L}$, the METT attaching to the skin will withstand an average strain (ε)

$$\varepsilon = \frac{L-L_0}{L_0} \tag{1}$$

According to the resistance equation, the resistance of the liquid metal-based strain sensor can be written as

$$R = \rho \frac{L}{A} \tag{2}$$

Here, L represents the length of the wire (in meters), ρ is the resistivity of the liquid metal (in ohm • meter), A is the cross-sectional area of the liquid metal strain sensor. We assume that the volume (V) of the liquid metal remains constant during stretching,

$$V = AL = constant \tag{3}$$

Thus the resistance of the strain sensor on the skin without crease can be written as

$$R = \rho \frac{L^2}{V} \tag{4}$$

In comparison, when stretching the skin with creases from $\boldsymbol{L_0}$ to $\boldsymbol{L}$, the METT will produce Crease Amplification Effect. In this model, all creases in the skin have the same properties. When stretching the skin, the strain will focus on METT above the creases. In contrast, we can ignore the deformation on the METT attached to the skin. Thus, the length (L_r) of the non-deformable area of the strain sensor on the METT can be written as

$$L_r = L_0 - anL_0 \tag{5}$$

Where a presents the initial length of the "suspended part" (in meters), n presents the density of the creases (in meters^{-1}). After stretching, the length of the strain sensor on the METT can be written as

$$L = L_r + a'nL_0 \tag{6}$$

In which, a' is the length of the "suspended part" after stretching (in meters). Due to the Crease Amplification Effect, the strain will focus on the "suspended part" of the METT. We obtain the strain (a') of the "suspended part" of the METT

$$a' = \frac{L-L_0}{nL_0} + a \tag{7}$$

So, the strain (ε') of the "suspended part" can be written as

$$\varepsilon' = \frac{a'-a}{a} \tag{8}$$

$$\varepsilon' = \frac{L/L_0-1}{na} \tag{9}$$

The resistance of the strain sensor on the skin with creases consists of two parts, the resistance of the non-deformable part (R_r) and the resistance of the "suspended part" (nL_0R_s). Thus, the resistance (R') after stretching can be written as

$$R' = R_r + nL_0R_s \tag{10}$$

In which, R_r presents the resistance of the non-deformable parts while R_s presents the resistance of a single "suspended part". According to the resistance equation, R_r and R_s can be written as

$$R_r = \rho \frac{{L_r}^2}{\frac{L_r}{L_0}V} \tag{11}$$

$$R_s = \rho \frac{{a'}^2}{\frac{a}{L_0}V} \tag{12}$$

Combining equation (5) (7) (10) (11) (12), we can obtain the resistance of the strain sensor caused by the Crease Amplification Effect when stretching to a length of L.

$$R' = \frac{\rho(L-L_0)^2}{anV} + \frac{\rho(2L_0L-L_0^2)}{V} \tag{13}$$

We obtain the increased value in resistance of the strain sensor caused by the Crease Amplification Effect.

$$R' - R = \frac{\rho(L-L_0)^2}{anV} + \frac{\rho\left(2L_0L-L_0^2\right)}{V} - \rho\frac{L^2}{V} \tag{14}$$

$$R' - R = \frac{\rho(L-L_0)^2}{V}\left(\frac{1}{an} - 1\right) \tag{15}$$

So we obtain the equation of the Crease Amplification Effect.

$$\frac{R'-R}{R} = \varepsilon^2\left(\frac{1}{an} - 1\right) \tag{16}$$

In which, ε is the average strain of the strain sensor, a is the initial length of the "suspended part", n presents the density of the creases.

The 1-layered METT can increase the resistance of the strain sensors on the PIP to about 3 times that of strain sensors under average strains (Fig. 2). The density of the creases on the PIP is about 0.4 mm^{-1}. The average strain (ε) of the strain sensor when bending the PIP to 105 degrees is about 40% (Fig. 2). According to formula (16), we can obtain the initial length (a) of the "suspended part" is about 0.2 mm. According to formula (9), So the strain of the "suspended part"(ε') (local strain) of the strain sensor is about 500%.

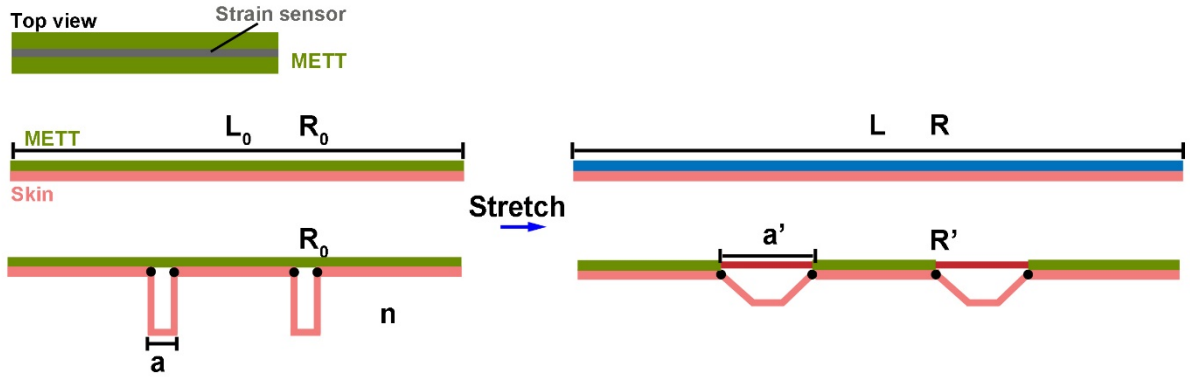

Fig. S1. A model shows the stretching of the METT on the skin with and without creases. The METT on the skin without crease is under an average strain. The METT on the skin with creases has large local deformation on the crease, while there is no deformation outside the creases.

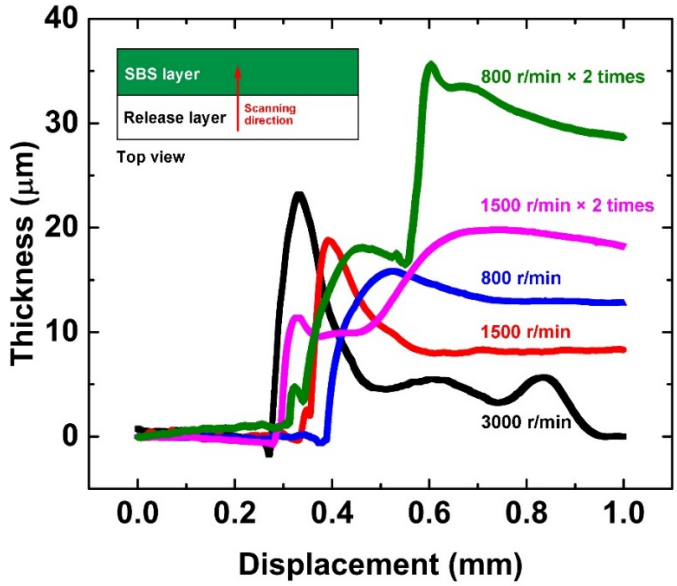

Fig. S2. Measurements of the thickness of the SBS layer. The thickness of the SBS layer after spin-coating for different speeds and times. Inset, the scanning direction of the probe.

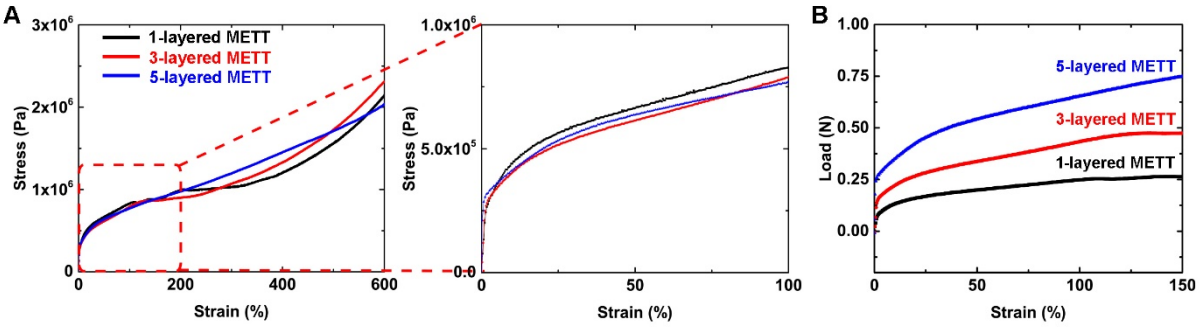

Fig. S3. The stress-strain curve of the METT with different layers. (A) The METT with different layers has a similar strain-stress curve when the strain is less than 100%. (**B**) The load-strain curve of the METT with different layers.

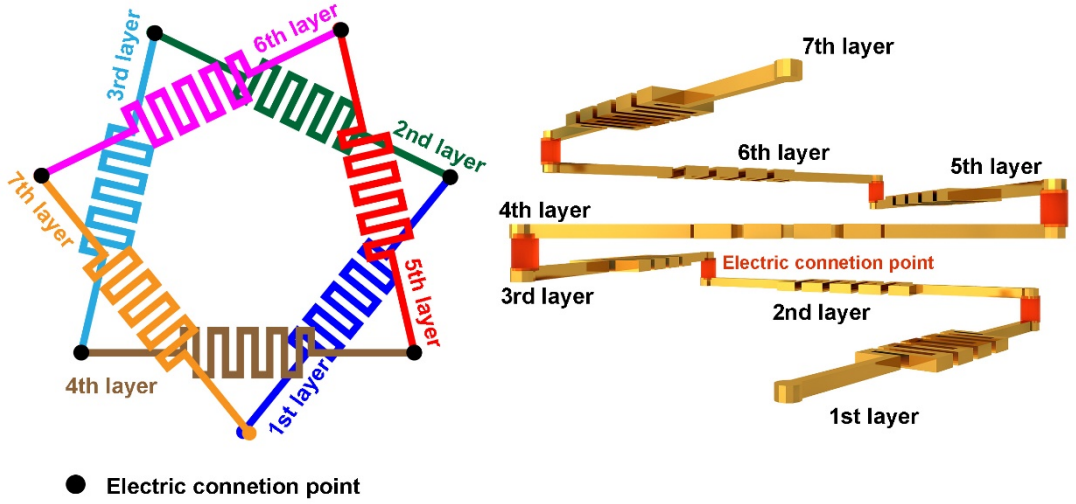

Fig. S4. Schematic illustrations of the 7-layered heater based on the METT. (Left) The top view of the 7-layered heater. (Right) The cross-section of the 7-layered heater.

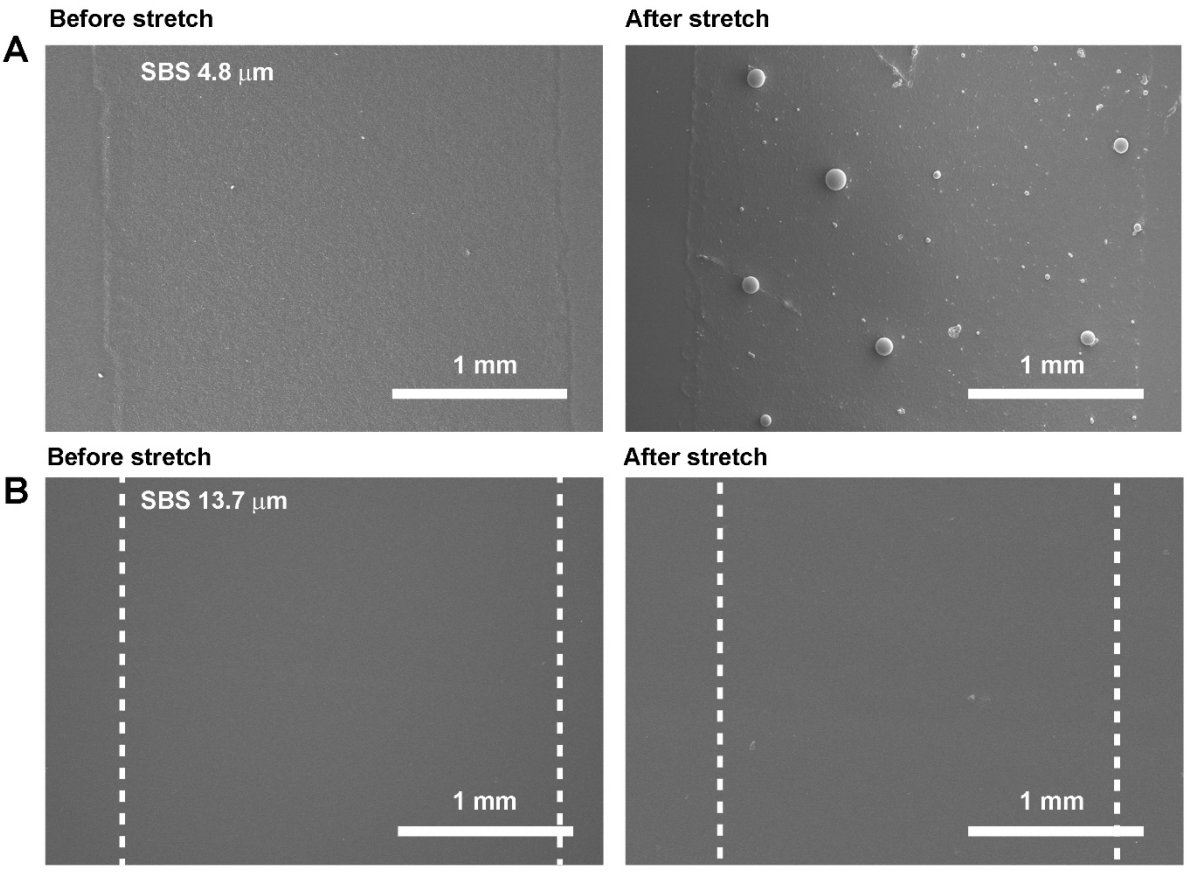

Fig. S5. SEM characterization of the surface of the SBS layer before and after stretch. (**A**) SBS layer with a thickness of 4.8 μm. (**B**) SBS layer with a thickness of 13.7 μm. Dotted line, the sealed MPC.

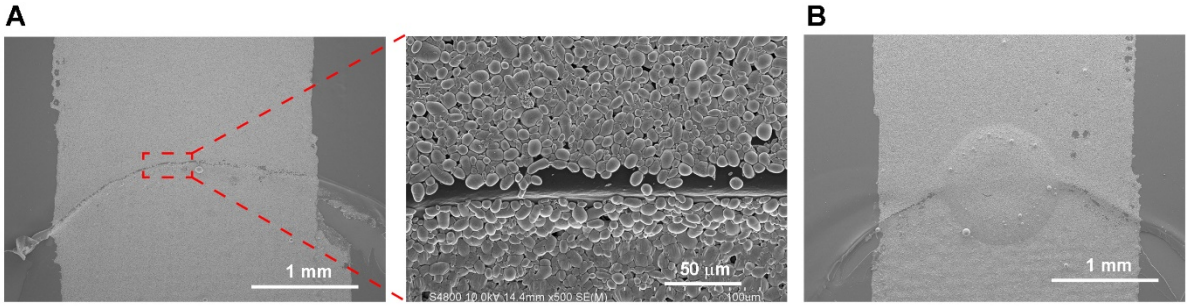

Fig. S6. Characterization of the edge of the electric connection point. (A) The electric connection point with a depth of 18.1 μm, which blocks the MPC paths. (B) We add an extra drop of MPC ink on the edge of the electric connection point for connections of the MPC in different layers.

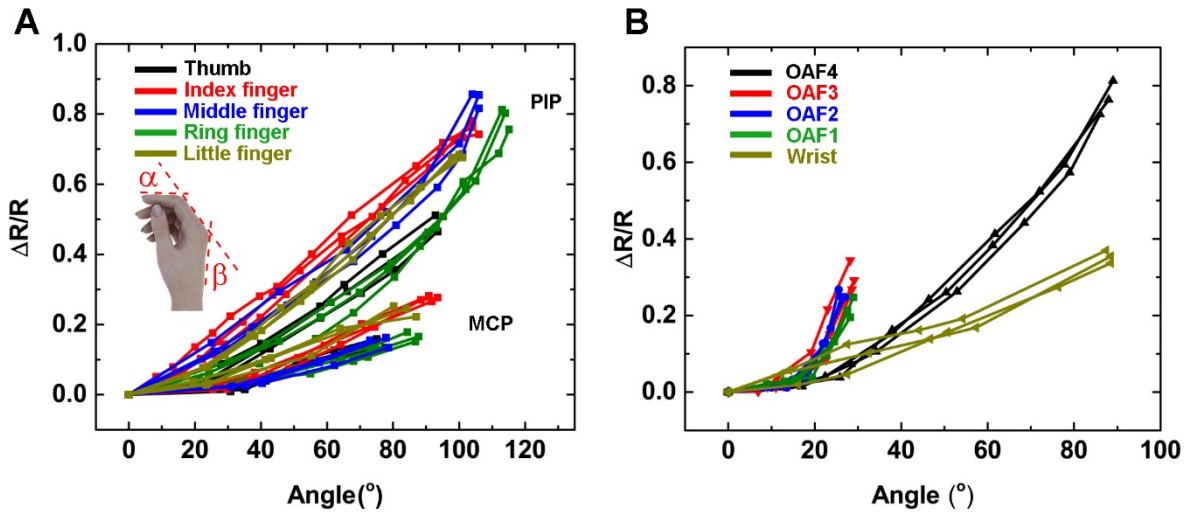

Fig. S7. Monitoring the movements of the hand using the 3-layered METT. (**A**) ΔR/R of strain sensors versus bending angles of the PIP and MCP in each finger. (**B**) ΔR/R of strain sensors versus open angles of the fingers and bending angle of the wrist. (Photo credit: Lixue Tang, Southern University of Science and Technology.)

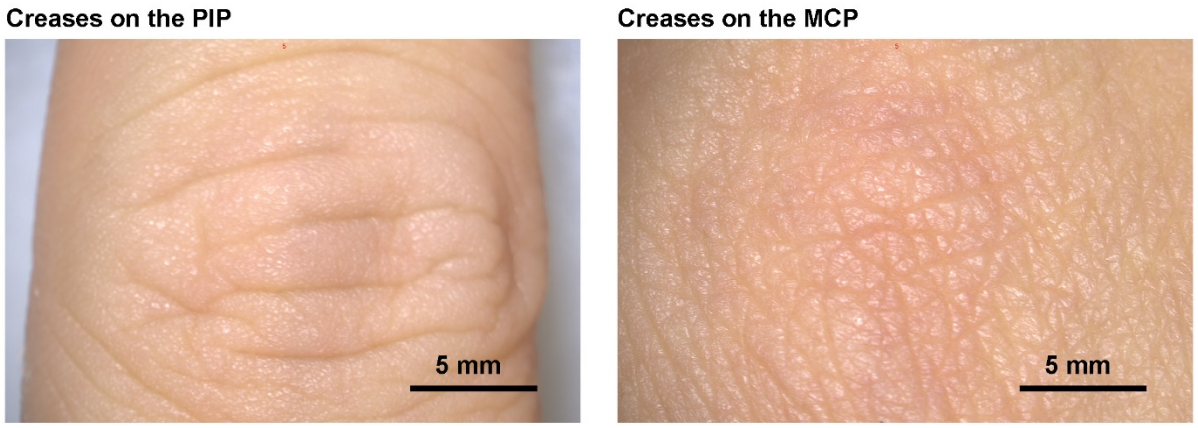

Fig. S8. Optical image of the creases on the PIP and MCP. The MCPs (~ 1.3 mm^{-1}) have a larger density of creases than that of PIPs (~ 0.4 mm^{-1}). (Photo credit: Lixue Tang, Southern University of Science and Technology.)

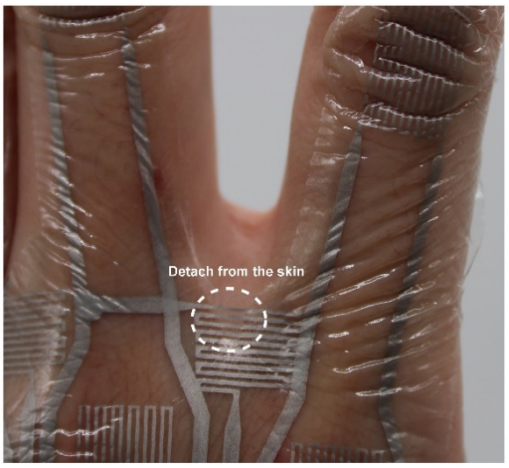

Fig. S9. Photograph of the METT on the OAF when splaying the finger. Some of the parts on the strain sensor between two fingers will detach during deformations. (Photo credit: Lixue Tang, Southern University of Science and Technology.)

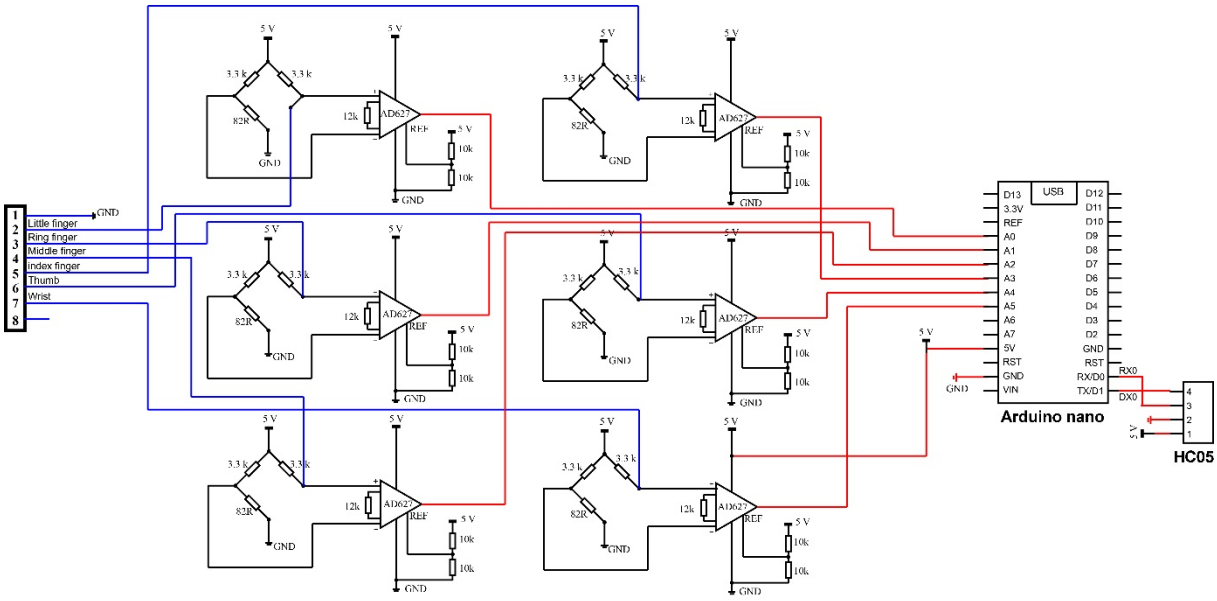

Fig. S10. The circuit design of the robot controlling system. The system includes a signal processing module that contains 6 Wheatstone bridges and 6 instrumental amplifiers (AD627), a Bluetooth module (HC-05), and a controller (Arduino nano).